In Vivo ^{1}H MR Spectroscopy in the Evaluation of the Serial Development of Hepatocarcinogenesis in an Experimental Rat Model[1]

Hui Xu, Ph.D., Xuan Li, M.D., Zheng-han Yang, M.D., Jing-xia Xie, M.D.

Rationale and Objectives. We used a 1.5-T MR scanner to investigate in vivo hydrogen 1 (^{1}H) MRS to evaluate metabolic changes in the hepatocarcinogenesis experimental rat model.

Materials and Methods. Hepatocellular carcinoma (HCC) was induced by diethylnitrosamine in 70 treated rats with 20 normal rats used as controls. Single-voxel ^{1}H MRS is performed to obtained the relative choline-to-lipid (Cho/lipid) ratio. The liver and tumor tissues are incised for the histologic examination. Based on the histologic result, the progression of hepatocarcinogenesis of the animal model was divided into three stages: fibrosis stage, cirrhosis stage, and HCC stage. The mean (±SD) ratio values are calculated and compared at various stages between the treated group and the control group.

Results. In control group, the calculated mean (±SD) Cho/lipid ratio was 0.15 ± 0.05. With the progression of hepatocarcinogenesis, the Cho/lipid ratio increased significantly, to 0.18 ± 0.05, 0.24 ± 0.07, and 0.38 ± 0.19, respectively.

Conclusion. The ^{1}H MRS is technically feasible for evaluation of the metabolic changes in the animal model. A significant increase in choline-containing compounds level was observed in the HCC stage in the treated group.

Key Words. In vivo ^{1}H magnetic resonance spectroscopy; hepatocellular carcinoma; animal model

Hepatocellular carcinoma (HCC) is the most common primary malignant tumor of the liver, with highest incidence in Africa, Southeast Asia, and China. Worldwide, it is thought to result in over 1 million deaths every year and is increasing (1,2). The major risk factor for HCC is cirrhosis. All types of cirrhosis predispose to HCC, but the incidence is particularly high in persistent infection of hepatitis B and hepatitis C viruses, and in alcoholic liver disease (3–5). Hepatocellular carcinogenesis in patients with cirrhosis is a continuum multistep de-differentiation process from benign regenerative nodule via dysplastic nodule to HCC (6–8).

Orthotopic liver transplantation (OLT) is widely accepted as effective therapeutic modality for patients with end-stage cirrhosis and HCC. It has been reported (9) that long-term survival can be achieved with OLT in patients with a solitary HCC of 5 cm or smaller in diameter or tumor nodules of 3 cm or smaller in diameter. Nevertheless, one may not wish to perform OLT in a cirrhotic patient if advanced HCC is present. Therefore, it is important to screen liver transplant candidates for HCC to determine their eligibility for transplantation, especially in light of the shortage of donor livers.

Although imaging techniques have improved during the past two decades, screening for HCC in cirrhotic liver is still challenging. Screening of high-risk cirrhotic patients is usually made through the use of ultrasound, high or increasing serum levels of α-fetoprotein, computed tomography, magnetic resonance imaging (MRI), and bi-

Acad Radiol 2006; 13:1532–1537

[1] From the Department of Radiology, Peking University Third Hospital, 49 North Garden Road, Haidian District, Beijing, 100083, P. R. China (H.X., X.L., J.-x.X.); the department of Radiology, Beijing Hospital, Beijing 100730, P.R. Ching (Z.-h.Y.). This work was supported by the Nature and Science Foundation of Beijing (No. 7063091). Received August 10, 2006; accepted September 1, 2006. **Address correspondence to:** X.L. e-mail: dubu_xiyang@yahoo.com.cn; xuanli@vip.sina.com

doi:10.1016/j.acra.2006.09.001

opsy. In recent reports based on thin section of whole explanted livers, the sensitivity and specificity of helical computed tomography and MRI are still lower in detecting small HCC or dysplastic nodules (10–14). The most accurate and reliable diagnostic method of HCC is needle biopsy of the liver. However, liver biopsy has limitations, such as a high false-negative rate, mental discomfort of patients, and possibility of spread of the tumor along the needle track.

Therefore, the need for a noninvasive diagnostic method for the early detection of HCC is critical. MRS enables the noninvasive measurement of biochemical information and metabolic changes in vivo. In vivo ^{1}H MRS has been used successfully in the diagnosis of tumors in the brain (15,16), prostate (17,18), and breast (19), and the usefulness of MRS in evaluating the effectiveness of chemotherapy has been reported in tumors (20–22). In the liver, ^{1}H MRS has been proved useful in evaluating diffuse hepatic disease such as hepatic steatosis, chronic hepatitis, and cirrhosis (23,24).

MRS can be used to monitor biochemical changes that continue to occur throughout tumor development and progression in colorectal carcinoma and in HCC (25–27). Foley (26) found (by using a 7.0-T MR) that the lipid components had changed in the serial development of hepatocarcinogenesis in an experimental rat model. It should be noted that this study used 7.0-T MR, which is not proved to be safe for clinical research at the present. To our knowledge, few investigations (22,27) have used a clinical MR scanner to distinguish benign from malignant lesions in the cirrhotic liver; uncertainties still exist and further studies are necessary.

In our study, we sought to test the feasibility of ^{1}H MRS in evaluation of the biochemical information of rat liver by use of a clinical 1.5-T MR. Furthermore, we evaluated the metabolic changes of the serial development of hepatocarcinogenesis in an experimental rat model.

MATERIALS AND METHODS

Animal Model

This experiment was performed in accordance with the *Guide for the Care and Use of Laboratory Animals* (National Institutes of Health publication No. 85-23, revised 1996), with the approval of the local ethical committee for animal care and use.

The 6-week-old male Sprague-Dawley (SD) rats (n = 90) weighing 120–150 g were supplied by the Department of Laboratory Animal Science, Peking University, China. The animals were acclimated for 1 week and maintained under specific pathogen-free (SPF) environmental conditions with lights on from 9:00 a.m. to 9:00 p.m., temperature of 22 ± 2°C, and relative humidity of 45–60%. They were fed chow pellets and solution ad libitum during the entire study period.

All rats were divided into two groups: 70 were used for HCC induction with 70 mg/kg diethylnitrosamine (DEN, 0.95 g/ml; Sigma Chemical, St. Louis, MO) intragastrically once a week for 10 weeks. Twenty normal rats were used as controls.

MRI Studies

From week 7 to week 20 after induction with by DEN, four or five treated animals and one to three control animals were scanned randomly every week. Before imaging, rats were fasted for 12 hours and then anesthetized with 40 mg/kg pentobarbiral sodium (Nembutal; Beijing Chemical Co., Beijing, China) intraperitoneally.

The rats were examined with a 1.5-T whole-body MR system (Sonata; Siemens, Erlangen, Germany) with a maximum gradient capability of 40 mT/m and maximum slew rate of 150 T/m/s. A two-channel phased-array coil (the coil is specially designed for rat with a diameter of 5 cm; Chen Guang Medical Science Co., Shanghai, China) was used for all MRI. The rats were placed in the supine position inside the coil with the liver region located in the center of the coil and the abdomen fixed with adhesive tape to reduce respiratory movement.

Conventional liver MR protocols were as follows: (1) TSE (turbo spin-echo) T2-weighted axial, sagittal, and coronal orientations (TR = 3000 ms, TE = 79 ms, a flip angle of 150°, field of view 90 mm × 65 mm, matrix 192 × 135, slice thickness 3 mm); (2) axial orientation FLASH-2D (fast low-angle shot) T1-weighted images (TR = 250 ms, TE = 3.53 ms, a flip angle of 70°, field of view 90 mm × 55 mm, matrix 192 × 135, slice thickness 3 mm).

The single-voxel MRS using a water-suppressed point-resolved spectroscopy sequence (PRESS, SVS-SE-30; Siemens Medical Systems) was performed with TR = 1500 ms; TE = 30 ms; number of averages = 192; voxel size = 10 mm × 10 mm × 10 mm; and 1024 data points. The acquisition time was 4 minutes 56 seconds. The location of the voxel of interest (VOI) was performed by a single experienced radiologist specialized in gastrointestinal and hepatic MRI. Using the axial, sagittal, and coronal T2WI images, the VOI was located in the tumor

or obviously nodular concentrated areas. MRS was undertaken in an area within the middle portion of the right hepatic lobe, avoiding the large intrahepatic vessels in control and no-nodular rats.

Histology

The animals were killed after the last set of MR studies. The liver and tumor tissues were obtained and fixed in 4% buffered formalin. The samples were obtained at the same position as the VOI of MRS, embedded in paraffin. Thin sections of 5 μm were cut and stained with hematoxylin-eosin for histologic examination.

Data Analysis

According to the histologic findings, the serial progression of hepatocarcinogenesis of the animal model was divided into three stages: fibrosis stage (weeks 7–11), cirrhosis stage (weeks 12–14), and HCC stage (weeks 15–20).

MRS data were analyzed using commercially available software (Spectroscopy; Siemens Medical Systems) by a single MR physicist who was experienced in MRS analysis. The MRS data with serious baseline distortion, which makes it very difficult to recognize the lipid resonance and the choline-containing compounds resonance, were excluded from our analysis. We obtained the relative choline-to-lipid (Cho/lipid) ratio by dividing the peak area of the choline-containg compounds at 3.2 ppm by the peak area of lipid at 0.9–1.4 ppm. The mean ($\pm$SD) ratio values were calculated at various stages of animal model and the control group.

Data were first evaluated using one-way analysis of variance (ANOVA), and then LSD post-hoc tests were used to determine the different mean Cho/lipid ratio among groups by statistical software (SPSS for Windows, Version 12; SPSS Inc, Chicago, IL). A two-tailed P-value of less than 0.05 was required for statistical significance.

RESULTS

Seven treated rats died of the hemorrhage of the tumor or overdose of anesthesia before imaging. Then the number of the rats that finished the whole experiment was 83. In all cases, we successfully obtained 61 (73.5%, 61 of 83) eligible ^{1}H MRS curves: 48 treated rats (11 in fibrosis stage, 16 in cirrhosis stage, and 21 in HCC stage) and 13 control rats. The other 22 rats were excluded from analysis because of unsatisfied MRS (those with serious baseline distortion, which makes it very difficult to recognize the lipid resonance and the choline-containing compounds resonance).

According to the histologic findings, in the treated rats, histologic changes in the fibrosis stage (weeks 7–11) include local steatosis, hepatocellular vacuolation, and bridging fibrosis between the two portal veins or between the portal vein and the central vein in the liver. In the cirrhosis stage (weeks 12–14), pseudolobes surrounded by collagen fibers, which is typical for cirrhosis, were widely observed in the liver, and numerous regenerative nodules and fewer dysplastic foci and dysplastic nodules could be seen in this stage. The cells of dysplastic foci or dysplastic nodules are usually different from those of adjacent hepatocytes with respect to cytoplasmic staining, nuclear size, or degree of nuclear atypia. Nuclei may be normal in size or large and hyperchromatic. There is a spectrum of nuclear atypia from minimal to severe. The cytoplasmic contents of fat may be more or less than the surrounding liver. The nuclear-cytoplasmic ratio is normal or slightly increased, and the liver plates are one or two cells wide or more than two cells wide. A nodule-in-nodule pattern may be seen when small dysplastic nodules are present within the cirrhotic nodule. The prominent changes after 15 weeks in the treated rats were the genesis of HCC, which is more prominent after 16 weeks. Small foci of HCC also could be seen arising within dysplastic nodules. Both necrosis and hemorrhage are common in advanced tumors. There was normal architecture of hepatic lobule in the control rats liver.

The large peak at ^{1}H MRS occurred at 0.9–1.4 ppm, where the chemical shift of the lipid occurs; another peak was choline-containing compounds at 3.2 ppm. In control group, the calculated mean ($\pm$SD) Cho/lipid ratio was 0.15 ± 0.05. With hepatocarcinogenesis progress of the animal model, the Cho/lipid ratio increased significantly (Fig. 1); the ratios at the fibrosis stage, cirrhosis stage, and HCC stage were 0.18 ± 0.05, 0.24 ± 0.07, and 0.38 ± 0.19, respectively (Fig. 2). There was a statistically significant difference between fibrosis stage with HCC stage ($P < .05$), between cirrhosis stage with HCC stage ($P < .05$), between cirrhosis stage with the control group ($P < .05$), and between HCC stage and the control group ($P < .05$). However, there was no significant difference either between the control group and the treated group at the fibrosis stage ($P > .05$) or between the fibrosis stage and the cirrhosis stage ($P > .05$).

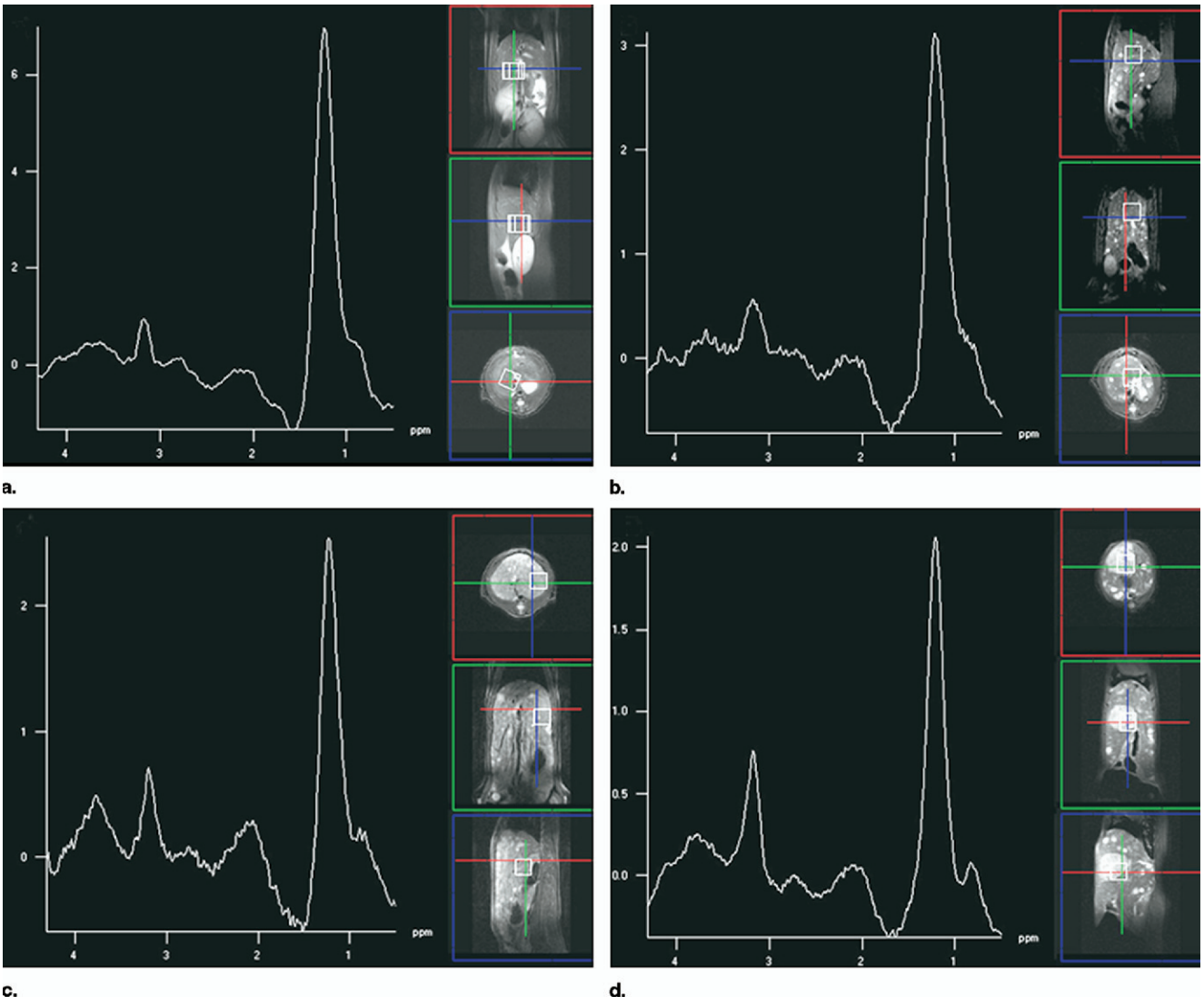

Figure 1. *A–D,* T2WI axial, sagittal, and coronal images as references and MRS curves. The ¹H MRS of the liver showed that lipid compounds peak at 0.9–1.4 ppm and Cho (choline-containing compounds) peak at 3.2 ppm. With the progression of the animal model, the Cho/lipid ratio increased significantly. *A,* Control rat. *B,* Fibrosis stage rat. *C,* Cirrhosis stage rat. *D,* HCC stage rat; the location of the voxel in the tumor, which was pathologically proved to be an HCC.

DISCUSSION

At present, ¹H MR spectroscopy at liver is still challenging. Physiologic motion due to respiratory motion and cardiac movement may increase background noise and further hinder the detection of small amounts of metabolites within the liver, especially when the VOI is located in the left hepatic lobe or extreme end of the right hepatic lobe. In our study, the ¹H MR spectrum of the liver demonstrates the lipid peak at 0.9–1.4 ppm and choline-containing compounds peak at 3.2 ppm. The ¹H MRS is technically feasible for evaluation of the metabolic changes in the experimental rat model. Of the MRS curves, 73.5% (61 of 83) was considered technically satisfactory and eligible for calculating the Cho/lipid ratio. In the HCC stage of the treated rats, there is apparent hepatomegaly and the liver can occupy the majority of the abdomen, which could help the localization of VOI and increase the signal-to-noise ratio to some degree. Incorporating the experience of Zhao and colleagues (27), we use appropriate deeper anesthesia to control the respiration and obtain the satisfactory results at last.

At ¹H MR spectroscopy, the choline-containing compounds (resonance at 3.2 ppm) include choline, phospho-

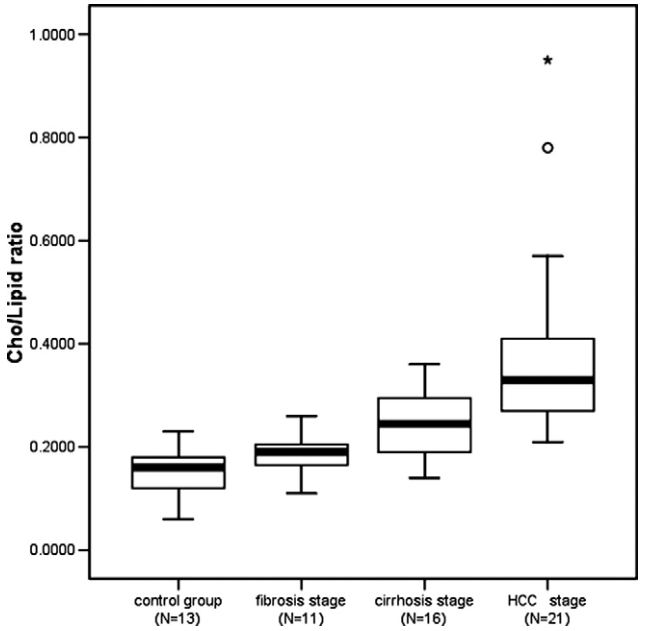

Figure 2. Graph illustrates the Cho/lipid ratio at control group and the various stages of the rat model. Significant values among the groups for the Cho/lipid ratio: control vs. fibrosis stage ($P = 0.512$); fibrosis stage vs. cirrhosis stage ($P = 0.215$); control vs. cirrhosis stage ($P = 0.046$); control vs. HCC stage ($P < 0.001$); fibrosis stage vs. HCC stage ($P < 0.001$); cirrhosis stage vs. HCC stage ($P = 0.001$)

choline, glycerophosphocholine, and taurine (28,29). At the magnetic field strengths of 1.5 T, these multiple resonances appear as a single peak and cannot be distinguished. Choline and its derivatives are thought to represent important constituents in the phospholipid metabolism of cell membranes (30). Elevation of the choline peak is thought to represent increased membrane phospholipid biosynthesis; therefore, it could be used as an active marker for cellular proliferation that occurs with the evolution and progression of malignant tumors (30–33).

Previous research (34–36) has indicated that in vivo ^{1}H MRS can be used to differentiating malignant lesions from benign lesions based on quantitative measurement of choline-containing compounds (Cho). Tumors after chemotherapy show a decreased choline level (20,22). In our study, the histologic features of this DEN-induced animal model simulate the progression of hepatocarcinogenesis in human cirrhotic liver and are a result of sequential steps from regenerative nodules via dysplastic nodules (37). In the HCC stage of the treated rats, the Cho/lipid ratio increased significantly compared with the control group, the fibrosis stage, and the cirrhosis stage. This phenomenon may reflect the increased cellular proliferation and cell density with the hepatocarcinogenesis. Our study also showed that a choline resonance was present in normal liver, which was similar to the study of Lim (28). However, the mean concentration was relatively low owing to the lower cell turnover in normal liver.

Cho and colleagues (24) found ^{1}H MRS was useful in grading the severity of fibrosis in chronic hepatitis. However, in our study, although the Cho/lipid ratio increased from the cirrhosis stage to the fibrosis stage, there is no statistically significant difference between these two stages. Considering that there was an overlap in the distribution of ratios between these two stages and that MRS detects biochemical rather than structural changes, this finding was reasonable, since cirrhotic liver and fibrosis tissue has not lost its functionality in some degree. Another explanation for our result is that the speed of the hepatocarcinogenesis was very fast and this process produces a continuous spectrum of abnormality, so there are overlaps in histologic characteristics in these two stages. That is why we cannot obtain a statistically significant difference between them.

Our study had some limitations. One of the major limitations is a relatively large, single voxel size of 10 mm × 10 mm × 10 mm that we used. With the hepatocarcinogenesis progress of the animal model, the dysplastic nodules and HCC nodules were usually smaller than the voxel; the VOI of MRS contains not only nodules but also the peripheral relatively normal tissue. In addition, we could not precisely distinguish the necrotic and hemorrhage part from the viable one in HCC; contamination error therefore cannot avoided. Although we observe that in the HCC stage of the animal model, the choline levels increase significantly, the results cannot be used to screen HCC in a high-risk population of cirrhosis. Despite its limitation, this research suggests that further studies with a larger number of patients are still essential to resolve the problem.

There is another limitation in this study. Because the lack of external reference, we used lipid as internal reference to quantify the choline-containing compounds with the ratio method. However, the lipid varies in different pathologies: Foley and colleagues (26) found that the integral of the lipid increased significantly in the early period of treated groups and then dropped to the same level as controls in a long-term HCC animal model induced by DEN. Similarly, Zhao (27) found the lipid level to be changed in different periods of a short-term DEN-induced rat model. Therefore, to prevent the influence of lipid changed in different pathologies, the external reference

will be necessary for further MRS studies to demonstrate the actual change in the metabolites.

In conclusion, the ^{1}H MRS is noninvasive and technically feasible for evaluating the metabolic changes of the serial development of hepatocarcinogenesis in the experimental HCC rat model. A significant increase in choline-containing compound level was seen in the HCC stage in the treated group. The in vivo ^{1}H MRS may have a potential capability in screening for HCC among the high-risk group of cirrhosis patients.

REFERENCES

1. Unoura M, Kaneko S, Matsushita E, et al. High-risk groups and screening strategies for early detection of hepatocellular carcinoma in patients with chronic liver disease. Hepatogastroenterology 1993; 40:305–310.
2. Parkin DM. Global cancer statistics in the year 2000. Lancet Oncol 2001; 2:533–543.
3. Kasahara A, Hayashi N, Mochizuki K, et al. Risk factors for hepatocellular carcinoma and its incidence after interferon treatment in patients with chronic hepatitis C. Osaka Liver Disease Study Group. Hepatology 1998; 27:1394–1402.
4. Tsai JF, Jeng JE, Ho MS, et al. Effect of hepatitis C and B virus infection on risk of hepatocellular carcinoma: A prospective study. Br J Cancer 1997; 76:968–974.
5. Benvegnu L, Gios M, Boccato S, Alberti A. Natural history of compensated viral cirrhosis: A prospective study on the incidence and hierarchy of major complications. Gut 2004; 53:744–749.
6. Terminology of nodular hepatocellular lesions. International Working Party. Hepatology 1995; 22:983–993.
7. Kojiro M. Focus on dysplastic nodules and early hepatocellular carcinoma: An Eastern point of view. Liver Transpl 2004; 10:S3–S8.
8. Efremidis SC, Hytiroglou P. The multistep process of hepatocarcinogenesis in cirrhosis with imaging correlation. Eur Radiol 2002; 12:753–764.
9. Mazzaferro V, Regalia E, Doci R, et al. Liver transplantation for the treatment of small hepatocellular carcinomas in patients with cirrhosis. N Engl J Med 1996; 334:693–699.
10. Earls JP, Theise ND, Weinreb JC, et al. Dysplastic nodules and hepatocellular carcinoma: Thin-section MR imaging of explanted cirrhotic livers with pathologic correlation. Radiology 1996; 201:207–214.
11. Lim JH, Kim CK, Lee WJ, et al. Detection of hepatocellular carcinomas and dysplastic nodules in cirrhotic livers: Accuracy of helical CT in transplant patients. AJR Am J Roentgenol 2000; 175:693–698.
12. Krinsky GA, Lee VS, Theise ND, et al. Hepatocellular carcinoma and dysplastic nodules in patients with cirrhosis: Prospective diagnosis with MR imaging and explantation correlation. Radiology 2001; 219:445–454.
13. Libbrecht L, Bielen D, Verslype C, et al. Focal lesions in cirrhotic explant livers: Pathological evaluation and accuracy of pretransplantation imaging examinations. Liver Transpl 2002; 8:749–761.
14. Rode A, Bancel B, Douek P, et al. Small nodule detection in cirrhotic livers: Evaluation with US, spiral CT, and MRI and correlation with pathologic examination of explanted liver. J Comput Assist Tomogr 2001; 25:327–336.
15. Law M, Cha S, Knopp EA, Johnson G, Arnett J, Litt AW. High-grade gliomas and solitary metastases: Differentiation by using perfusion and proton spectroscopic MR imaging. Radiology 2002; 222:715–721.
16. Law M, Yang S, Wang H, et al. Glioma grading: Sensitivity, specificity, and predictive values of perfusion MR imaging and proton MR spectroscopic imaging compared with conventional MR imaging. AJNR Am J Neuroradiol 2003; 24:1989–1998.
17. Scheidler J, Hricak H, Vigneron DB, et al. Prostate cancer: localization with three-dimensional proton MR spectroscopic imaging—Clinicopathologic study. Radiology 1999; 213:473–480.
18. Yu KK, Scheidler J, Hricak H, et al. Prostate cancer: Prediction of extracapsular extension with endorectal MR imaging and three-dimensional proton MR spectroscopic imaging. Radiology 1999; 213:481–488.
19. Yeung DK, Cheung HS, Tse GM. Human breast lesions: Characterization with contrast-enhanced in vivo proton MR spectroscopy—Initial results. Radiology 2001; 220:40–46.
20. Jagannathan NR, Kumar M, Seenu V, et al. Evaluation of total choline from in-vivo volume localized proton MR spectroscopy and its response to neoadjuvant chemotherapy in locally advanced breast cancer. Br J Cancer 2001; 84:1016–1022.
21. Schilling A, Gewiese B, Berger G, et al. Liver tumors: Follow-up with P-31 MR spectroscopy after local chemotherapy and chemoembolization. Radiology 1992; 182:887–890.
22. Kuo YT, Li CW, Chen CY, Jao J, Wu DK, Liu GC. In vivo proton magnetic resonance spectroscopy of large focal hepatic lesions and metabolite change of hepatocellular carcinoma before and after transcatheter arterial chemoembolization using 3.0-T MR scanner. J Magn Reson Imaging 2004; 19:598–604.
23. Longo R, Ricci C, Masutti F, et al. Fatty infiltration of the liver. Quantification by 1H localized magnetic resonance spectroscopy and comparison with computed tomography. Invest Radiol 1993; 28:297–302.
24. Cho SG, Kim MY, Kim HJ, et al. Chronic hepatitis: In vivo proton MR spectroscopic evaluation of the liver and correlation with histopathologic findings. Radiology 2001; 221:740–746.
25. Mackinnon WB, Huschtscha L, Dent K, Hancock R, Paraskeva C, Mountford CE. Correlation of cellular differentiation in human colorectal carcinoma and adenoma cell lines with metabolite profiles determined by 1H magnetic resonance spectroscopy. Int J Cancer 1994; 59:248–261.
26. Foley LM, Towner RA, Painter DM. In vivo image-guided (1)H-magnetic resonance spectroscopy of the serial development of hepatocarcinogenesis in an experimental animal model. Biochim Biophys Acta 2001; 1526:230–236.
27. Zhao WD, Guan S, Zhou KR, et al. In vivo detection of metabolic changes by 1H-MRS in the DEN-induced hepatocellular carcinoma in Wistar rat. J Cancer Res Clin Oncol 2005; 131:597–602.
28. Lim AK, Hamilton G, Patel N, Bell JD, Taylor-Robinson SD. H MR spectroscopy in the evaluation of the severity of chronic liver disease. Radiology 2003; 226:288–289.
29. Li CW, Kuo YC, Chen CY, et al. Quantification of choline compounds in human hepatic tumors by proton MR spectroscopy at 3 T. Magn Reson Med 2005; 53:770–776.
30. Dixon RM. NMR studies of phospholipid metabolism in hepatic lymphoma. NMR Biomed 1998; 11:370–379.
31. Lim AK, Patel N, Hamilton G, Hajnal JV, Goldin RD, Taylor-Robinson SD. The relationship of in vivo 31P MR spectroscopy to histology in chronic hepatitis C. Hepatology 2003; 37:788–794.
32. Ruiz-Cabello J, Cohen JS. Phospholipid metabolites as indicators of cancer cell function. NMR Biomed 1992; 5:226–233.
33. Mukherji SK, Schiro S, Castillo M, Kwock L, Muller KE, Blackstock W. Proton MR spectroscopy of squamous cell carcinoma of the extracranial head and neck: In vitro and in vivo studies. AJNR Am J Neuroradiol 1997; 18:1057–1072.
34. Jagannathan NR, Seenu V, Kumar M. Potential of in vivo proton MR spectroscopy in the assessment of breast lesions without the use of contrast agent. Radiology 2002; 223:281–282; author reply 282.
35. Katz-Brull R, Lavin PT, Lenkinski RE. Clinical utility of proton magnetic resonance spectroscopy in characterizing breast lesions. J Natl Cancer Inst 2002; 94:1197–1203.
36. Soper R, Himmelreich U, Painter D, et al. Pathology of hepatocellular carcinoma and its precursors using proton magnetic resonance spectroscopy and a statistical classification strategy. Pathology 2002; 34:417–422.
37. Ha WS, Kim CK, Song SH, Kang CB. Study on mechanism of multistep hepatotumorigenesis in rat: Development of hepatotumorigenesis. J Vet Sci 2001; 2:53–58.